AIAA JOURNAL
Vol. 47, No. 9, September 2009

Technical Notes

Flow Control Predictions Using Unsteady Reynolds-Averaged Navier–Stokes Modeling: A Parametric Study

Christopher L. Rumsey*
NASA Langley Research Center, Hampton, Virginia 23681-2199
and
David Greenblatt†
Technion—Israel Institute of Technology, 32000 Haifa, Israel

DOI: 10.2514/1.41855

I. Introduction

THE effective control of flow separation promises substantial performance improvements for a wide variety of air vehicles. Although the methods are well known, there is very little by way of theory or numerical models that can adequately predict lift enhancements, drag reduction, etc. An attempt was made to address this problem by conducting a computational fluid dynamics (CFD) validation workshop for synthetic jets and turbulent separation control [1], where one case was dedicated to predicting the nominally two-dimensional flow over a hump. The baseline (uncontrolled) case was considered in addition to control by means of steady suction [2] and zero-net-mass flux (oscillatory) blowing [3]. The workshop determined that CFD with steady or unsteady Reynolds-averaged Navier–Stokes (RANS or URANS) consistently overpredicted the reattachment location, regardless of turbulence model or method. Within the separation bubble, most computations predicted velocity profiles well but considerably underpredicted the magnitude of turbulent shear stresses. Large-eddy simulations and other costly methods appear capable of overcoming this deficiency, but the focus of the current study is on the more affordable RANS and URANS methodologies. See, for example, Krishnan et al. [4], Morgan et al. [5], and Saric et al. [6].

Although these individual test cases were challenging to CFD codes, only a single test case was considered for both steady suction and zero-net-mass flux blowing. During the course of the experimental investigation, however, steady and unsteady surface pressures were acquired for a wide variety of control parameters, including Reynolds number, suction flow rate, and frequency and blowing amplitude in the zero-net-mass flux case. Significant variations, or changes, in control authority were observed depending upon the control input or prevailing Reynolds numbers. For example, varying the suction flow rate at different Reynolds numbers indicated an increase in the rate of drag reduction; in contrast, no Reynolds number effect could be detected with regard to zero-net-mass flux blowing. In addition, for the oscillatory case, the flow was seen to be highly dependent on control frequency and peak blowing amplitude. Different, sometimes counteracting, mechanisms dominated the separated flowfield during different parts of the control cycle. Comparisons of these changes, or trends, with numerical results will clearly facilitate more precise evaluation of CFD's value for predictive purposes. This is because the uncontrolled, or baseline, state is usually known and hence the correct prediction of changes to the baseline state as a result of a particular control strategy would be of great value for assessing different concepts or downselection. To address this need, Rumsey and Greenblatt [7] undertook a detailed parametric study and this Note presents a summary of the main findings.

II. Results

A. Flowfield Conditions

The wall-mounted hump model had a chord of $c = 0.42$ m, height of 0.0538 m at its maximum thickness point, and width of 0.5842 m. The configuration was two dimensional, and experimental results were demonstrated to be nominally 2-D. The flow-control slot was located near 65% c; this was close to where the flow separated in its uncontrolled state. A summary of the flowfield conditions studied can be found in [7]. The freestream Mach number for all computations was $M = 0.1$. For the steady suction cases, the steady mass transfer momentum coefficient is defined by $c_\mu = \rho h U_j^2/(cq)$, where $h = 0.00187c$ is the slot height, U_j is the total jet velocity, and q is the freestream dynamic pressure. The c_μ corresponds with a steady mass flow rate (given by $\dot{m}$) through the slot. For the unsteady oscillatory cases, the oscillatory flow momentum coefficient is defined by $\langle c_\mu \rangle = \rho h \langle U_j \rangle^2/(cq)$, where $\langle U_j \rangle$ is the root mean square of the total jet velocity. The c_μ and $\langle c_\mu \rangle$ parameters are typically used in experiments to characterize flow-control blowing levels and are cited as percentages throughout this paper. Furthermore, for the oscillatory cases, the reduced excitation frequency is defined as $F^+ = fX/U_\infty$, where X is the distance from the slot to flow reattachment point for no flow control and U_∞ is the freestream velocity. Additional information concerning this case can be found on the Web site for the validation workshop.‡

B. Computational Details

The computer code employed was CFL3D [8], an upwind-biased, finite volume, structured Navier–Stokes solver that uses pseudotime stepping with multigrid and achieves second-order spatial and temporal accuracy. Three different turbulence models are used in the current study: the Spalart–Allmaras (SA) model [9], Menter's k–ω shear-stress transport (SST) model [10], and the nonlinear explicit algebraic stress model in k–ω form (EASM-ko) [11].

The 2-D computations used a fine-level 4-zone grid with 208,320 cells. The jet slot and cavity were included in the hump model computations. Many of the computations used a "medium-level" version of the grid consisting of every other point in each coordinate direction, or 52,080 cells. Several grid studies were performed, both here and as well as in previous work for the workshop cases [12]. These studies indicated that there were almost no differences between mean flow quantities (either long time averaged or phase averaged) on the two grid levels, and less than 5% difference in turbulence quantities. Time step studies were also performed for the oscillatory control case, and indicated that using at least 180 steps per period in conjunction with 20 subiterations per time step was sufficient to yield little perceptible change in results. For all results to

Received 28 October 2008; revision received 27 May 2009; accepted for publication 27 May 2009.

*Senior Research Scientist, Computational Aerosciences Branch, Mail Stop 128.
†Senior Lecturer, Faculty of Mechanical Engineering.

‡Data available online at http://cfdval2004.larc.nasa.gov. [retrieved September 2008].

be shown here, 360 steps per period were used. Details concerning the grid and boundary conditions can be found in [7]. A view of the hump geometry using a medium-level grid is shown in Fig. 1.

C. Results for Steady Suction

As mentioned earlier, historically all RANS methods applied to this case have yielded results with too long a separation bubble, because they underpredicted the magnitude of the turbulent shear stress in the separated region. In spite of this deficiency, we turn to the question of whether RANS is capable of predicting changes relative to the baseline state. Figure 2 gives surface pressure coefficients at $Re = 0.936 \times 10^6$ for a range of different c_μ coefficients (0.030, 0.076, 0.24, 0.47, and 0.73%). Only results with SA are shown here; SST and EASM-ko were reasonably similar, although SA tended to give the overall best agreement with experiment. The CFD exhibited a similar trend as experiment, but not all of the physical details were correctly modeled. Upstream of separation, the flow acceleration due to the steady suction was well predicted with increasing c_μ. Downstream of the separation point, the separation extent decreased similarly for CFD and experiment, but the CFD predicted a pressure increase downstream of the slot instead of a steeper pressure recovery observed in the experiment. Despite the qualitative difference, the models clearly predict the main overall effect, namely, a reduction of the bubble length.

In the experiment, Greenblatt et al. [2] noted a clear Reynolds number effect both at $c_\mu = 0.24\%$ and $c_\mu = 0.47\%$, despite the small Reynolds number range tested (from $Re = 0.557 \times 10^6$ to 1.1×10^6). Comparisons with a similar hump model [13] at a much higher Reynolds number of 16×10^6 showed a continuing Reynolds number effect, which was most evident when comparing form drag on the respective models. In the CFD results, there was also a clear trend of increasing effectiveness with increasing Reynolds number. The largest differences occurred below a Reynolds number of 16×10^6. This trend is shown in Fig. 3, which summarizes the effect

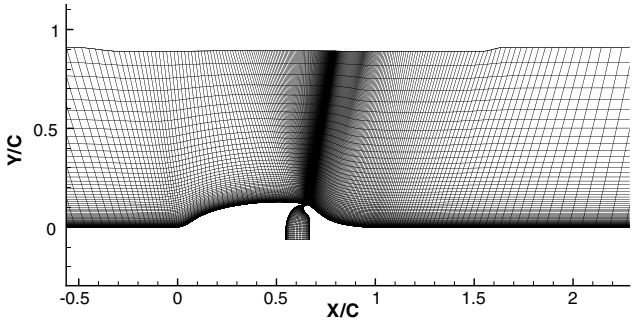

Fig. 1 View of hump geometry and medium-level grid (52,080 cells).

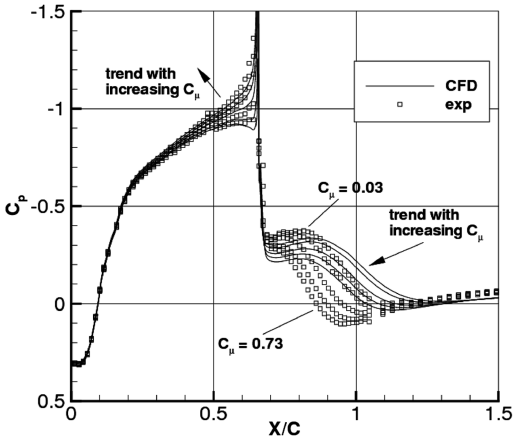

Fig. 2 Effect of c_μ (in %) on surface pressure coefficients for steady suction, $Re = 0.936 \times 10^6$; CFD shows results using the SA model.

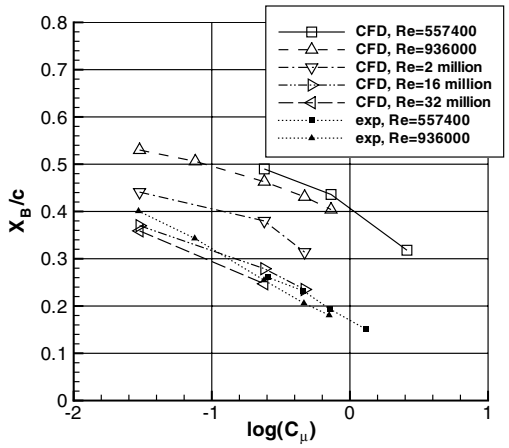

Fig. 3 Bubble length as a function of c_μ for steady suction; CFD shows results using the SA model.

of c_μ and the Reynolds number on bubble length (X_B/c). The only experimental data available, as determined by surface oil-film visualization, were at the lowest Reynolds numbers of 557,400 and 936,000. Here, the general trend of decreasing bubble length with increasing c_μ is evident. At these Reynolds numbers, there is an offset between the experimental data and numerical prediction, mainly due to the poor prediction of the baseline state. In the experiments, the bubble length decreased as $-\log(c_\mu)$, whereas the numerical predictions indicated a more effective shortening of the bubble at higher c_μ. Nevertheless, the changes in bubble length were similar at these two Reynolds numbers. The most dramatic shortening of the bubble, as predicted by the CFD, occurred when the Reynolds number was increased to 16×10^6, corresponding to a factor of nearly 30 relative to the lowest Reynolds number considered; a further doubling of the Reynolds number to 32×10^6 produced only small changes. These observations are consistent with earlier studies of boundary-layer control by means of steady suction [14]. Coincidentally, the X_B values from CFD at the highest Reynolds number matched fairly well with the experimental ones at the lowest Reynolds number.

RANS tended to underpredict the pressure drag coefficient (c_{dp}) by as much as 30% (not shown). To directly compare overall changes only, both the bubble length and form-drag results were calculated relative to the baseline state for $Re = 0.936 \times 10^6$ (Fig. 4). Although the approximate difference in bubble length is captured, it is evident that the rate at which the bubble length is shortened is not correctly predicted by any of the models. Moreover, none of the models properly captures the logarithmic variation evident in the experiment. The net result is that at low c_μ the SA and SST models agree better

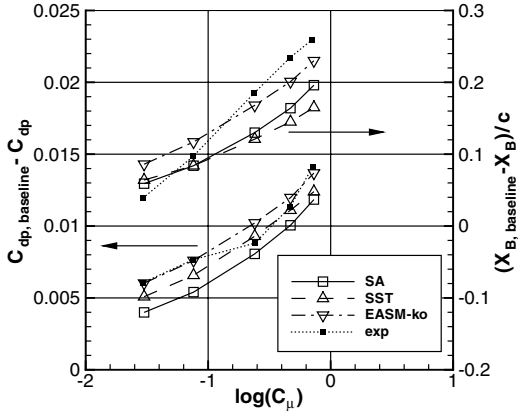

Fig. 4 Bubble length and pressure drag coefficient relative to the baseline (no control) as a function of c_μ for steady suction, $Re = 0.936 \times 10^6$.

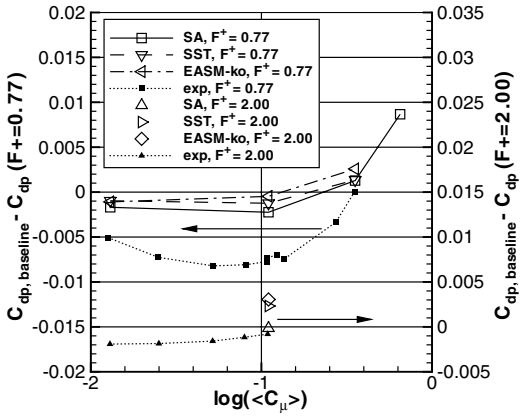

Fig. 5 Pressure drag coefficient relative to baseline (no control) as a function of $\langle c_\mu \rangle$ for oscillatory control; $Re = 0.936 \times 10^6$.

with experiment, while at high c_μ the EASM-ko model produces the best predictions. For c_{dp}, all three turbulence models appear capable of predicting the correct trends but the EASM-ko produced superior prediction throughout almost the entire c_μ range.

D. Results for Oscillatory Control

Similar to the steady suction condition, the long-time-averaged bubble size for the oscillatory control case was always overpredicted using URANS. However, as discussed by Rumsey [12] and Rumsey and Greenblatt [7], the relative motion of the large-scale convected vortical flow structures caused by the pulsed jet/suction were predicted qualitatively fairly well, in terms of their effect on phase-averaged surface pressures.

Unlike the steady suction case [2], no Reynolds number effect was observed in the zero-net-mass flux control experiments [3], provided that the dimensionless quantities F^+ and $\langle c_\mu \rangle$ were precisely matched. Given the small Reynolds number range considered, it is conceivable that there is a Reynolds number effect, but that this effect is much smaller than that associated with steady suction. CFD simulations were performed where the effect of Reynolds number and $\langle c_\mu \rangle$ were explored for oscillatory control (not shown). Between $Re = 0.936 \times 10^6$ and 16×10^6, CFD also exhibited a small increase of control effectiveness: the bubble length decreased from $X_B/c = 0.601$ to 0.536 and c_{dp} decreased slightly from 0.023 to 0.022. Hence the small Reynolds number effect predicted by the simulations indicated a qualitative agreement with the experimental data set. Although not shown, at a given Reynolds number the effects of varying F^+ in CFD only qualitatively reproduced some of the mean effects seen in experiment. Specifically, the control saturation effect with increasing frequency was attained, but the sharp pressure drop downstream of the slot at low $\langle c_\mu \rangle$ was not reproduced.

Figure 5 shows c_{dp} relative to the baseline state as a function of $\langle c_\mu \rangle$ for two different F^+ using all three turbulence models. Unlike the steady suction case for which CFD predicted the change relative to the baseline well, in this case the change was not captured accurately. In the experiment, when the peak jet blowing velocity was less than that in the freestream (corresponding to $\langle c_\mu \rangle < 0.11\%$), a separated region was promoted immediately downstream of the slot and this low pressure region produced the unexpected increase in c_{dp}. Irrespective of the turbulence model used, CFD results at low values of $\langle c_\mu \rangle$ did not capture this effect. At higher F^+, the difference between the three turbulence models was more pronounced than at lower F^+, with the SA agreeing best with experimental trends. Both the experimental data and the numerical simulations showed notable decreases in c_{dp} near and above $\langle c_\mu \rangle \approx 0.3\%$.

III. Conclusions

An extensive computational study was conducted with RANS and URANS and three different turbulence models in application to the hump model case from a flow-control validation workshop held in 2004. Many of these cases were not part of the workshop itself, but were included in the experiment. They included investigations into the effects of Reynolds number, control magnitude, and control frequency, and have not been computed before. The purpose of this study was to investigate the effectiveness of RANS and URANS CFD for predicting trends in this type of flow-control application, where it is already known to mispredict absolute levels.

In summary, all three turbulence models performed similarly, in the sense that differences between the models were generally much less than differences between CFD and experiment. For steady suction, CFD appeared capable of qualitatively predicting the effects of Reynolds number and c_μ, and this was clearly evident by comparing separation bubble length and form-drag changes. Nevertheless, the pressure recovery details were not correctly predicted. The fact that both experiment and CFD showed a strong Reynolds number effect is important because the majority of experiments are performed at low Reynolds number laboratory conditions ($Re \leq 1 \times 10^6$) and are assumed to remain valid under typical flight conditions with Reynolds number at several tens of millions.

For oscillatory control, the CFD indicated increasing effectiveness in the mean with increasing Reynolds number, but the effect was not nearly as pronounced as with steady suction. This was consistent with experimental data [3], but the experimental Reynolds number range was not large enough to draw firm conclusions. CFD was not able to reproduce many of the mean effects observed when varying oscillatory frequency and momentum. However, consistent with experimental data, a significant reduction in form drag was observed near and above $\langle c_\mu \rangle \approx 0.3\%$.

As is well known, steady RANS is deficient for predicting controlled separated flows, mostly because of the inability to accurately model turbulence in the separation/reattachment regions. The difficulty is compounded for URANS applied to oscillatory control, for which the nature of the Reynolds-averaged equations offers little hope of accurately resolving any but the largest scale unsteady features. Despite these misgivings, this investigation has shown that RANS (and to a lesser extent URANS) can qualitatively capture some of the trends in the hump model flow-control experiments. Thus, provided that absolute levels are not a primary metric, it can be justifiable to employ these approaches as a preliminary test for the feasibility of design changes.

References

[1] Rumsey, C., Gatski, T., Sellers, W., Vatsa, V., and Viken, S., "Summary of the 2004 Computational Fluid Dynamics Validation Workshop on Synthetic Jets," *AIAA Journal*, Vol. 44, No. 2, 2006, pp. 194–207. doi:10.2514/1.12957

[2] Greenblatt, D., Paschal, K. B., Yao, C.-S., Harris, J., Schaeffler, N. W., and Washburn, A. E., "Experimental Investigation of Separation Control Part 1: Baseline and Steady Suction," *AIAA Journal*, Vol. 44, No. 12, 2006, pp. 2820–2830. doi:10.2514/1.13817

[3] Greenblatt, D., Paschal, K. B., Yao, C.-S., and Harris, J., "Experimental Investigation of Separation Control Part 2: Zero Mass-Efflux Oscillatory Blowing," *AIAA Journal*, Vol. 44, No. 12, 2006, pp. 2831–2845. doi:10.2514/1.19324

[4] Krishnan, V., Squires, K. D., and Forsythe, J. R., "Prediction of Separated Flow Characteristics over a Hump," *AIAA Journal*, Vol. 44, No. 2, 2006, pp. 252–262. doi:10.2514/1.13174

[5] Morgan, P. E., Rizzetta, D. P., and Visbal, M. R., "High-Order Numerical Simulation of Turbulent Flow Over a Wall-Mounted Hump," *AIAA Journal*, Vol. 44, No. 2, 2006, pp. 239–251. doi:10.2514/1.13597

[6] Saric, S., Jakirlic, S., Djugum, A., and Tropea, C., "Computational Analysis of a Locally Forced Flow Over a Wall-Mounted Hump at High-Re Number," *International Journal of Heat and Fluid Flow*, Vol. 27, No. 4, 2006, pp. 707–720. doi:10.1016/j.ijheatfluidflow.2006.02.015

[7] Rumsey, C. L., and Greenblatt, D., "Parametric Study of Flow Control Over a Hump Model Using an Unsteady Reynolds-Averaged Navier-Stokes Code," NASA TM-2007-214897, Sept. 2007.

[8] Krist, S. L., Biedron, R. T., and Rumsey, C. L., "CFL3D User's Manual (Ver. 5.0)," NASA TM-1998-208444, June 1998.
[9] Spalart, P. R., and Allmaras, S. R., "A One-Equation Turbulence Model for Aerodynamic Flows," *Recherche Aerospatiale*, No. 1, 1994, pp. 5–21; also AIAA Paper 92-0439, 1992.
[10] Menter, F. R., "Two-Equation Eddy-Viscosity Turbulence Models for Engineering Applications," *AIAA Journal*, Vol. 32, No. 8, 1994, pp. 1598–1605.
doi:10.2514/3.12149
[11] Rumsey, C. L., and Gatski, T. B., "Summary of EASM Turbulence Models in CFL3D with Validation Test Cases," NASA TM-2003-212431, June 2003.
[12] Rumsey, C., "Reynolds-Averaged Navier-Stokes Analysis of Zero Efflux Flow Control Over a Hump Model," *Journal of Aircraft*, Vol. 44, No. 2, 2007, pp. 444–452.
doi:10.2514/1.23514
[13] Seifert, A., and Pack, L. G., "Active Flow Separation Control on Wall-Mounted Hump at High Reynolds Numbers," *AIAA Journal*, Vol. 40, No. 7, 2002, pp. 1363–1372.
doi:10.2514/2.1796
[14] Schlichting, H., *Boundary Layer Theory*, 7th ed., McGraw–Hill, New York, 1979.

J. Sahu
Associate Editor